Available online at www.sciencedirect.com
SCIENCE DIRECT®
Journal of Solid State Chemistry 177 (2004) 4535–4541
JOURNAL OF SOLID STATE CHEMISTRY
www.elsevier.com/locate/jssc

Synthesis crystal structure and ionic conductivity of $Ca_{0.5}Bi_3V_2O_{10}$ and $Sr_{0.5}Bi_3V_2O_{10}$

Digamber G. Porob, T.N. Guru Row*

Division of Chemical Sciences, Solid State and Structural Chemistry Unit, The Indian Institute of Science, Bangalore 560 012, India

Received 25 February 2004; received in revised form 10 August 2004; accepted 20 August 2004
Available online 11 November 2004

Abstract

Two new compounds $Ca_{0.5}Bi_3V_2O_{10}$ and $Sr_{0.5}Bi_3V_2O_{10}$ have been synthesized in the ternary system: MO–Bi_2O_3–V_2O_5 system ($M=M^{2+}$). The crystal structure of $Sr_{0.5}Bi_3V_2O_{10}$ has been determined from single crystal X-ray diffraction data, space group $P\bar{1}$ and $Z=2$, with cell parameters $a=7.1453(3)$ Å, $b=7.8921(3)$ Å, $c=9.3297(3)$ Å, $\alpha=106.444(2)^\circ$, $\beta=94.088(2)^\circ$, $\gamma=112.445(2)^\circ$, $V=456.72(4)$ Å^3. $Ca_{0.5}Bi_3V_2O_{10}$ is isostructural with $Sr_{0.5}Bi_3V_2O_{10}$, with, $a=7.0810(2)$ Å, $b=7.8447(2)$ Å, $c=9.3607(2)$ Å, $\alpha=106.202(1)^\circ$, $\beta=94.572(1)^\circ$, $\gamma=112.659(1)^\circ$, $V=450.38(2)$ Å^3 and its structure has been refined by Rietveld method using powder X-ray data. The crystal structure consists of infinite chains of (Bi_2O_2) along c-axis formed by linkage of BiO_8 and BiO_6 polyhedra interconnected by MO_8 polyhedra forming 2D layers in ac plane. The vanadate tetrahedra are sandwiched between these layers. Conductivity measurements give a maximum conductivity value of 4.54×10^{-5} and 3.63×10^{-5} S cm^{-1} for $Ca_{0.5}Bi_3V_2O_{10}$ and $Sr_{0.5}Bi_3V_2O_{10}$, respectively at 725 °C.

Keywords: Bismuth vanadates; Crystal structure; Rietveld refinement; Ionic conductivity

1. Introduction

The bismuth vanadate, $Bi_4V_2O_{11}$, belonging to the Aurivillius family, has attracted much attention as the *parent phase* for a family of oxide ion conductors known as BIMEVOX [1,2]. During the study of Na_2O–Bi_2O_3–V_2O_5 system, Sinclair et al. [3] isolated a new compound $NaBi_3V_2O_{10}$ first in M_2O–Bi_2O_3–V_2O_5 ternary system. The structure of $NaBi_3V_2O_{10}$ is built of $(Bi_2O_2)^{2+}$ chains extended along the c-axis with the vanadium tetrahedra acting as linkers between chains [4,5]. The usual arrangement of BiO_4 units forming $(Bi_2O_2)^{2+}$ sheets in two dimension in Aurivillius family is restricted to a one-dimensional chain in $NaBi_3V_2O_{10}$. It is obvious that substitution of one Bi atom by a monovalent cation Na, in $Bi_4V_2O_{11}$ system has a major effect on the crystal structure and generates new and intricate motifs. It can therefore be anticipated that the $(Bi_2O_2)^{2+}$ layers can be modified using systematic substitution approach to replace Bi atoms by other monovalent or divalent metal atoms for a rational design of new materials. Hence, in order to find new structural types and stable phases, we have been investigating systems like M_2O–Bi_2O_3–X_2O_5 and $M'O$–Bi_2O_3–X_2O_5 where M and M' are univalent and divalent cations, respectively. In recent years there has been extensive study on bismuth-based phosphates and vanadate in the ternary systems $M'O$–Bi_2O_3–X_2O_5 (M' = divalent cations and X = P, V, As) [6–22]. Compounds in the series $PbBi_6X_4O_{20}$ (X = P, V, As) have been reported in the literature [19]. This series corresponds to $M_{0.5}Bi_3X_2O_{10}$ where $M=Pb^{2+}$ as compared to $NaBi_3V_2O_{10}$. In order to explore the potential of this system in generating novel structural types and study their conductivity properties, $M'_{0.5}Bi_3V_2O_{10}$ series with M' = Mg, Ca, Sr and Ba were studied. However, only two compounds $Ca_{0.5}Bi_3V_2O_{10}$ and $Sr_{0.5}Bi_3V_2O_{10}$ could be isolated as of a single phase. Attempts to synthesize

*Corresponding author. Fax: +91-80-2360-1310.
E-mail address: ssctng@sscu.iisc.ernet.in (T.N. Guru Row).

0022-4596/$ - see front matter © 2004 Elsevier Inc. All rights reserved.
doi:10.1016/j.jssc.2004.08.035

$Mg_{0.5}Bi_3V_2O_{10}$ and $Ba_{0.5}Bi_3V_2O_{10}$ by similar solid-state synthesis route were unsuccessful. Here we report the synthesis, crystal structure and conductivity of two new compounds belonging to $M'O$–Bi_2O_3–V_2O_5 system, namely $Ca_{0.5}Bi_3V_2O_{10}$ and $Sr_{0.5}Bi_3V_2O_{10}$.

2. Experimental

$Ca_{0.5}Bi_3V_2O_{10}$ and $Sr_{0.5}Bi_3V_2O_{10}$ (hereafter CBVO and SBVO, respectively) were prepared by conventional solid-state synthesis method. Bi_2O_3, V_2O_5, $CaCO_3$ and $SrCO_3$ (all AR grade) reagents were dried at 300 °C for 24 h and stored in a desiccator prior to use. The reaction mixtures of respective stoichiometries were weighed from the starting reagents, ground together in an agate mortar and pestle and fired in a platinum crucible at 600 °C for 3 days. To obtain single phase, regrinding and refiring process was repeated twice at 750 °C. Both the compounds were obtained as yellow powders. These compounds on heating above 800 °C start decomposing with $Bi_4V_2O_{11}$ appearing as a major phase. In order to monitor the decomposition behavior of CBVO and SBVO, independent fractions of the compound were heated at temperatures from 750 to 950 °C for 1 h at increments of 25° and powder XRD patterns of all these recorded. Some of these powder patterns are shown in Figs. 1 and 2. The appearance of $Bi_4V_2O_{11}$-related phase during the decomposition of CBVO and SBVO is clearly evident in samples heated at and above 800 °C. CBVO completely decomposes ca. 850 °C forming a $Bi_4V_2O_{11}$-related phase and hence single crystals of this phase could not be grown. However, the decomposition of SBVO is not complete even after melting (ca. 900 °C) and only a fraction of it decomposes. The single crystals of SBVO were grown by melting the product in a platinum crucible at 925 °C and slowly cooling the melt to room temperature at rate of 6 °C/h. The EDAX analysis on the crystallites confirmed the composition of crystals in the desired ratio. Single crystal X-ray diffraction data for SBVO were collected on a Bruker AXS SMART APEX CCD area detector [Mo$K\alpha$, $\lambda = 0.7107$ Å]. The initial unit cell was determined using a least squares analysis of a random set of reflections collected from three sets of 0.3° wide ω scans (50 frames/set) that were well distributed in reciprocal space. Data frames were collected with 0.3° wide ω-scans, 10 s per frame, 606 frames per set. Four complete sets were collected, using a crystal-to-detector distance of 6.03 cm, thus providing a complete sphere of data. The final unit cell parameters were obtained and refined using all the reflections. The SMART [23] software was used for data acquisition and SAINT [23] for data integration. High-resolution PXRD data for CBVO and SBVO were collected on a STOE/STADI-P X-ray powder diffractometer with Germanium monochromated Cu$K\alpha_1$ ($\lambda = 1.54056$ Å) radiation from a sealed tube X-ray generator (30 kV, 25 mA) in the transmission mode using a linear PSD ($2\theta = 3$–$100°$ with a step size of 0.02° with 8 s/step exposure time) at room temperature. The sample was rotated during the data collection to minimize preferred orientation effects, if any. The program TREOR90 in CRYSFIRE [24] package was used to index the PXRD pattern of CBVO and SBVO,

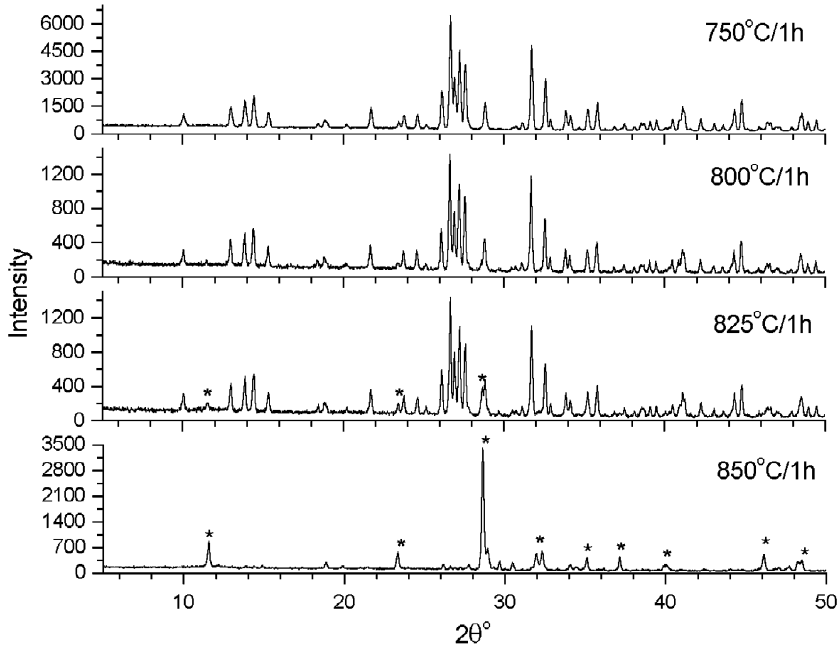

Fig. 1. PXRD patterns of $Ca_{0.5}Bi_3V_2O_{10}$ preheated at different temperatures. Reflections marked as (*) are due to $Bi_4V_2O_{11}$-related phase.

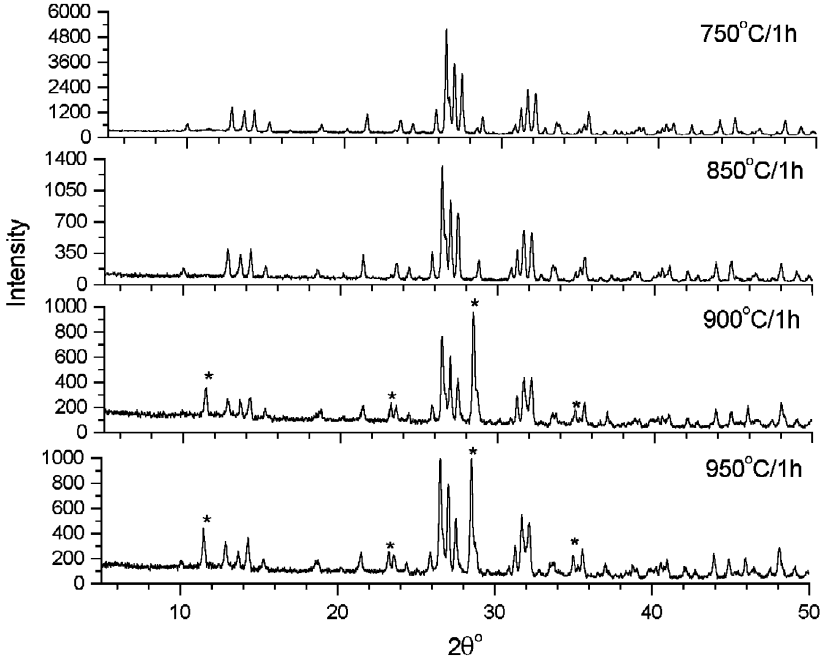

Fig. 2. PXRD patterns of $Sr_{0.5}Bi_3V_2O_{10}$ preheated at different temperatures. Reflections marked as (*) are due to $Bi_4V_2O_{11}$-related phase.

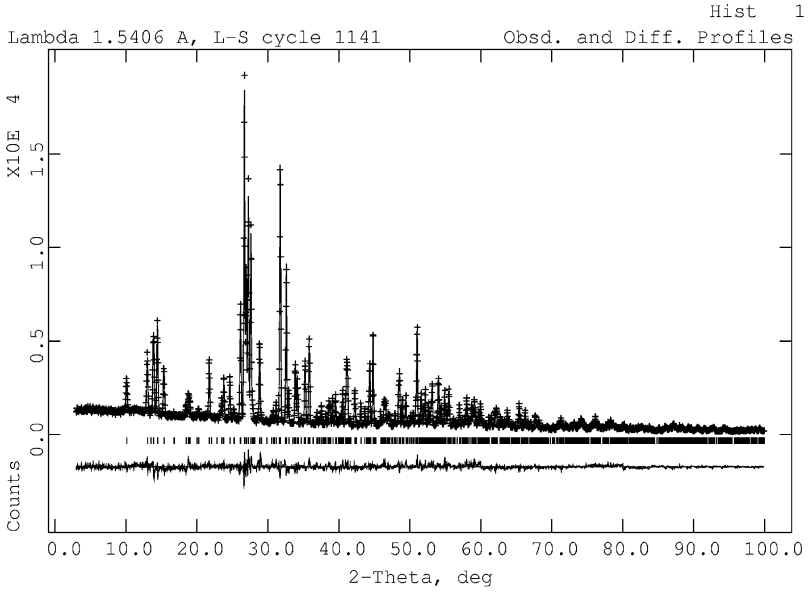

Fig. 3. Observed, calculated and difference X-ray diffraction patterns of $Ca_{0.5}Bi_3V_2O_{10}$.

which gave a triclinic cell equivalent to that obtained for SBVO from single crystal X-ray diffraction.

2.1. Structure of SBVO from single crystal data

The structure determination of SBVO was satisfactorily achieved in space group $P\bar{1}$. The structure was solved by direct methods using SHELXS97 [25] module in the WinGX [26] suite of software. Positions of three bismuth atoms and one strontium atom were obtained from the Fourier map. Two vanadium and 10 oxygen atoms were located by subsequent difference Fourier synthesis. Positional parameters and anisotropic displacement parameters of all the atoms were refined using SHELXL97 [25].

2.2. Structure of CBVO from powder X-ray data

The powder pattern of CBVO and its unit cell matched well with that of SBVO indicating it to be

isostructural to SBVO. Hence positional parameters of SBVO were used as the starting model for CBVO in the Rietveld refinement of PXRD data using GSAS [27]. The profile was fitted using Pseudo-Voigt function. A Chebyshev function consisting of 10 coefficients was used to define the background. The thermal parameters of all bismuth atoms were refined independently during the early stages of refinement. Since the Uiso values did not deviate much from each other, they were constrained to a single value and refined. A similar approach was used for vanadium and calcium atoms. The displacement parameters of all oxygen atoms were constrained together and refined. The occupancies of all the atoms were refined alternately with the thermal parameters. Since the occupancies did not deviate significantly from unity (full occupancy), the occupancy of all atoms was fixed at a value of 1.0. The observed, difference and calculated patterns are shown in Fig. 3.

2.3. Ionic conductivity measurements

Ionic conductivity was measured on a sintered pellet (sintered at 750 °C for 12 h) coated with gold paste using a HP4194A impedance/Gain phase analyzer over the frequency range 100 Hz–15 MHz in the temperature range 100–725 °C in air. The measurements were made for both heating and cooling cycles. The sample was equilibrated at constant temperature for about 30 min prior to each impedance measurement and the conductivity was obtained from the low-frequency intercept of the impedance plots.

3. Results and discussion

The experimental details pertaining to data collection and refinement are given in Table 1. The final positional and thermal parameters are given in Tables 2 and 3. ORTEP for SBVO with 50% probability level is shown in Fig. 4. The bond lengths and bond valence sum for SBVO are given in Table 4. CBVO and SBVO are isostructural to $PbBi_6X_4O_{20}$ (X = P, V, As) and $M_{0.5}Bi_3P_2O_{10}$ series (M = Ca, Sr, Ba, Pb) [19,22]. Packing diagram of SBVO viewed down the c-axis is shown in Fig. 5. The environment of oxygen atoms around Bi(1), Bi(2), Bi(3) and Sr in SBVO are shown in Fig. 6. The Bi(1) and Bi(3) atoms are coordinated to six oxygen atoms forming BiO_6 polyhedra. The $6s^2$ lone pair effect on these bismuth atoms is clearly evidenced by the distorted geometry of these polyhedra. In SBVO the Bi(1) atom has five relatively short bonds (2.145–2.536 Å) with O(1), O(1)′, O(3), O(7), O(8) on one side while O(9) forms a long bond (2.709 Å) on the other side which would host the lone pair. A similar coordination is observed in case of Bi(3). The five oxygen atoms O(1), O(2), O(4), O(9) and O(10) form five

Table 1
Crystallographic data for $Sr_{0.5}Bi_3V_2O_{10}$

Crystal data	
Chemical formula	$Sr_{0.5}Bi_3V_2O_{10}$
Formula weight	932.63
Crystal system	Triclinic
Space group	$P\bar{1}$
a (!Å)	7.106(5)
b (Å)	7.850(6)
c (Å)	9.277(7)
α (°)	106.43(1)
β (°)	94.12(1)
γ (°)	112.52(1)
V (Å^3)	449.0(6)
Z	2
D_x (Mg m^{-3})	6.90
Radiation type	Mo$K\alpha$
μ (mm^{-1})	63.581
Temperature (K)	293(2)
Crystal form, colour	Block, yellow
Crystal size (mm)	0.10 × 0.10 × 0.08
Data collection	
Diffractometer	Bruker AXS SMART APEX CCD area detector
Data collection method	ω scan
No. of measured, independent and observed reflections	5107, 2077, 1879
Criterion for observed reflections	$I > 2\sigma(I)$
R_{int}	0.034
θ range (°)	2.36-28.0
Range of h, k, l	$-9 \rightarrow h \rightarrow 9$ $-10 \rightarrow k \rightarrow 10$ $-11 \rightarrow l \rightarrow 12$
Refinement	
Refinement on	F^2
$R[I>2\sigma(I)]$, w$R([I>2\sigma(I)])$, S	0.052, 0.151, 1.068
$(\Delta/\sigma)_{max}$	0.004
$\Delta\rho_{max}$, $\Delta\rho_{min}$ (e Å^3)	6.309/−3.325

Table 2
Final atomic coordinates and isotropic thermal parameters from single crystal X-ray data for $Sr_{0.5}Bi_3V_2O_{10}$

Atom[a]	Site	x	y	z	U_{eq} (Å^2)
Bi1	2i	0.6545(1)	0.3724(1)	0.4852(1)	0.0209(2)
Bi2	2i	0.4248(1)	0.2938(1)	0.0792(1)	0.0209(2)
Bi3	2i	0.1989(1)	0.2086(1)	0.6716(1)	0.0196(2)
V1	2i	1.0524(4)	0.7730(4)	0.7585(3)	0.0183(5)
V2	2i	0.3428(4)	0.8970(4)	0.2596(3)	0.0174(5)
Sr	1c	0.000	0.500	0.000	0.0413(8)
O1	2i	0.555(2)	0.536(2)	0.372(1)	0.020(2)
O2	2i	0.105(2)	0.740(2)	0.274(2)	0.025(3)
O3	2i	1.235(2)	0.683(2)	0.759(2)	0.026(3)
O4	2i	0.331(2)	0.411(2)	0.895(2)	0.024(3)
O5	2i	0.862(2)	0.656(2)	0.849(2)	0.026(3)
O6	2i	0.349(2)	0.814(2)	0.074(2)	0.030(3)
O7	2i	0.371(2)	1.136(2)	0.316(2)	0.024(3)
O8	2i	0.952(2)	0.712(2)	0.572(2)	0.030(3)
O9	2i	0.533(2)	0.878(2)	0.366(1)	0.024(3)
O10	2i	1.162(2)	1.027(2)	0.839(2)	0.029(3)

[a]Occupancy = 1 for all the atoms.

Table 3
Anisotropic thermal parameters from single crystal X-ray data for $Sr_{0.5}Bi_3V_2O_{10}$

Atom	U_{11}	U_{22}	U_{33}	U_{23}	U_{13}	U_{12}
Bi1	0.0179(4)	0.0226(4)	0.0200(3)	0.0054(3)	0.0014(2)	0.0079(3)
Bi2	0.0260(4)	0.0282(4)	0.0342(4)	0.0114(3)	0.0097(3)	0.0110(3)
Bi3	0.0151(3)	0.0203(3)	0.0183(3)	0.0027(2)	−0.0001(2)	0.0056(2)
Sr1	0.063(2)	0.0073(9)	0.0247(12)	0.0022(8)	−0.0354(12)	−0.0054(10)
V1	0.0159(13)	0.0181(13)	0.0174(13)	0.0038(10)	0.0034(10)	0.0051(10)
V2	0.0139(12)	0.0193(13)	0.0172(12)	0.0045(10)	0.0023(10)	0.0064(10)
O1	0.023(6)	0.018(5)	0.019(5)	0.006(5)	0.003(5)	0.011(5)
O2	0.020(6)	0.027(6)	0.026(6)	0.008(5)	0.005(5)	0.008(5)
O3	0.020(6)	0.033(7)	0.027(6)	0.009(5)	0.005(5)	0.014(5)
O4	0.023(6)	0.026(6)	0.016(6)	0.006(5)	0.001(5)	0.004(5)
O5	0.017(6)	0.028(6)	0.029(7)	0.011(5)	0.005(5)	0.006(5)
O6	0.033(7)	0.041(8)	0.017(6)	0.010(5)	0.004(5)	0.016(6)
O7	0.018(6)	0.021(6)	0.030(6)	0.004(5)	−0.004(5)	0.009(5)
O8	0.031(7)	0.040(8)	0.021(6)	0.008(6)	0.002(5)	0.017(6)
O9	0.022(6)	0.027(6)	0.021(6)	0.005(5)	0.002(5)	0.011(5)
O10	0.027(7)	0.021(6)	0.035(7)	0.010(5)	0.004(6)	0.006(5)

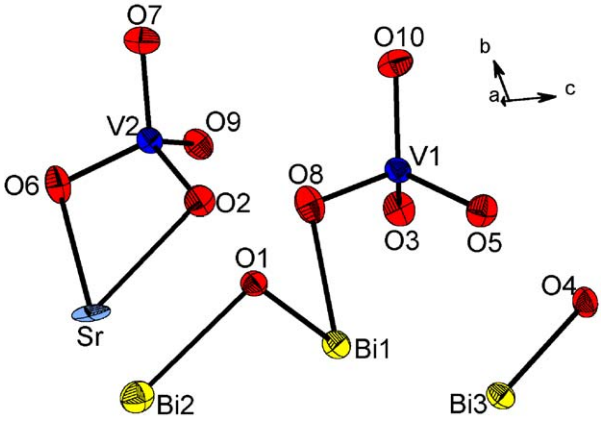

Fig. 4. ORTEP of $Sr_{0.5}Bi_3V_2O_{10}$ (50% probability).

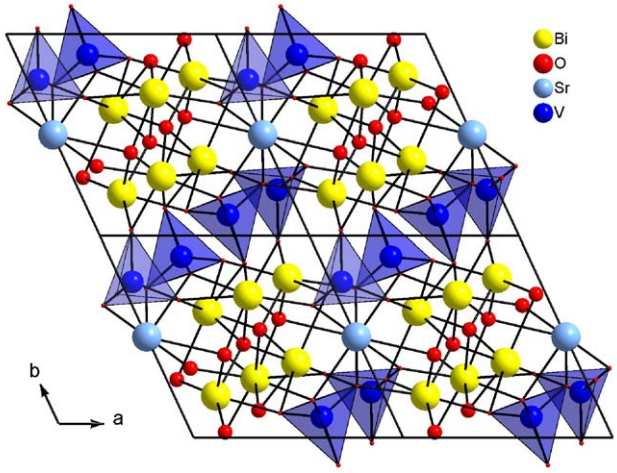

Fig. 5. Crystal structure of $Sr_{0.5}Bi_3V_2O_{10}$ viewed down the *c*-axis.

relatively short bonds (2.105–2.403 Å) on one side while O(8) forms a long bond (2.758 Å) on the other which would host the lone pair. Similar coordination features are observed in the case of CBVO. The Bi(2) and Ca/Sr cations are bonded to eight oxygen atoms. The BiO_8 coordination is highly distorted with two distinct types of bond lengths as observed in other bismuth atoms, a clear signature of the lone pair effect. The *M* atom occupies a special position and is coordinated to eight oxygen atoms, two each of O(2), O(4), O(5) and O(6) forming distorted MO_8 polyhedron. It is noteworthy that the *M* atom has a high anisotropic thermal parameter as compared to the Bi atoms (Fig. 4). A similar situation has been reported in the structures of $Bi_{6.67}P_4O_{20}$ and $M_{0.5}Bi_3P_2O_{10}$ series (*M* = Ca, Sr, Ba, Pb) [6,9]. The V(1) and V(2) atoms occupy the central interstitial of regular vanadate tetrahedra. The crystal structure can be described as built of (Bi_2O_2) chains interlinked via *M* cations forming a slab with VO_4 tetrahedra residing in between these slabs (Fig. 5). (Bi_6O_4) block forms a basic repeat unit of the chain formed by O(1), O(4) and bismuth atoms. The (Bi_6O_4) blocks are interconnected through two symmetry-related oxygen atoms O(4) and O(4)′, resulting in the formation of an infinite (Bi_2O_2) chain which extends along the *c*-axis. The *M* cation then links the (Bi_2O_2) chains in *ac* plane forming a slab by bonding to the O(4) atom of each chain.

The conductivity measurements in the form of Arrhenius plot ($\log\sigma$ vs. $1000/T$) are shown in Fig. 7 for both CBVO and SBVO. The Arrhenius plot shows a nearly linear increase of conductivity with temperature till ~600 °C. Above 600 °C, the conductivity shows a sharp linear increase with temperature. However, there is no accompanying phase transition as observed in

Table 4
Bond lengths and bond valence sum for $Sr_{0.5}Bi_3V_2O_{10}$

Atoms	Bond length (Å)	Bond valence
Bi1–O1	2.145(11)	0.871
Bi1–O1′	2.249(12)	0.658
Bi1–O3	2.432(13)	0.401
Bi1–O7	2.236(12)	0.681
Bi1–O8	2.536(15)	0.303
Bi1–O9	2.709(13)	0.190
Bond valence sum		3.104
Bi2–O1	2.686(12)	0.202
Bi2–O3	2.667(13)	0.213
Bi2–O4	2.231(13)	0.691
Bi2–O4′	2.323(13)	0.539
Bi2–O5	2.326(13)	0.534
Bi2–O6	2.450(14)	0.382
Bi2–O7	2.798(13)	0.149
Bi2–O10	2.568(14)	0.278
Bond valence sum		2.988
Bi3–O1	2.262(12)	0.635
Bi3–O2	2.403(13)	0.434
Bi3–O4	2.105(12)	0.971
Bi3–O8	2.758(13)	0.166
Bi3–O9	2.273(13)	0.616
Bi3–O10	2.354((14)	0.495
Bond valence sum		3.317
M–O2 × 2	2.552(13)	0.309
M–O4 × 2	2.860(13)	0.135
M–O5 × 2	2.467(13)	0.389
M–O6 × 2	2.610(15)	0.265
Bond valence sum		2.196
V1–O3	1.699(13)	1.325
V1–O5	1.744(13)	1.173
V1–O8	1.682(13)	1.387
V1–O10	1.742(13)	1.179
Bond valence sum		5.064
V2–O2	1.711(13)	1.282
V2–O6	1.668(13)	1.440
V2–O7	1.724(13)	1.238
V2–O9	1.692(13)	1.350
Bond valence sum		5.310

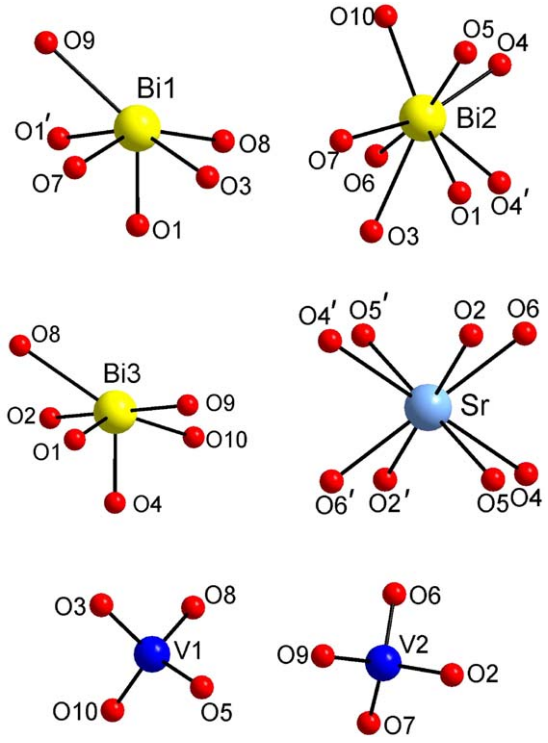

Fig. 6. Metal coordination in $Sr_{0.5}Bi_3V_2O_{10}$.

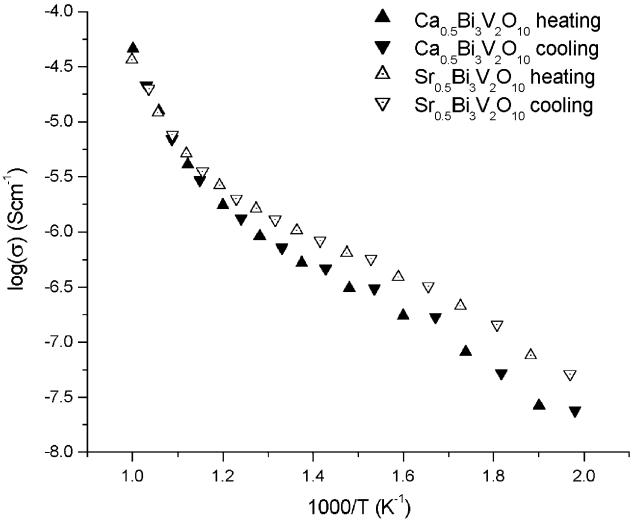

Fig. 7. Arrhenius plot for conductivity of CBVO and SBVO.

both HT-XRD and DTA data around this temperature. The conductivity values of 4.54×10^{-5} and 3.63×10^{-5} S cm^{-1} for $Ca_{0.5}Bi_3V_2O_{10}$ and $Sr_{0.5}Bi_3V_2O_{10}$, respectively, were obtained at 725 °C. These values few orders of magnitude lower from those found in Bismuth vanadates belonging to the BIMEVOX family (1). It is noteworthy that most of these structures have disorder in vanadium and oxygen atom sites, a likely reason for these materials to display high ionic conductivity. In the current study, the low-conductivity values may be due to the absence of any such disorder. The conductivity observed in CBVO and SBVO is likely to be oxide-ionic, as generally observed in case of bismuth vanadate systems.

Acknowledgments

The authors thank the Department of Science and Technology, India, for data collection on the CCD facility setup under the IRHPA-DST program and Professor A.K. Shukla for providing conductivity facility. Digamber Porob thanks CSIR, New Delhi, for the award of fellowship.

References

[1] J.C. Boivin, G. Mairesse, Chem. Mater. 10 (1998) 2870.
[2] K.R. Kendall, C. Navas, J.K. Thomas, H.C. Zur Loye, Chem. Mater. 8 (1996) 642.
[3] D.C. Sinclair, C.J. Watson, R.A. Howie, J.M.S. Skakle, A.M. Coats, C.A. Kirk, E.E. Lachowski, J. Marr, J. Mater. Chem. 8 (2) (1998) 281.
[4] D.G. Porob, T.N. Guru Row, Chem. Mater. 12 (2000) 3658.
[5] R. Bliesner, S. Uma, A. Yokochi, A.W. Sleight, Chem. Mater. 13 (2001) 3825.
[6] J. Huang, A.W. Sleight, J. Solid State Chem. 100 (1992) 170.
[7] J. Huang, Q. Gu, A.W. Sleight, J. Solid State Chem. 105 (1993) 599.
[8] I. Radosavljevic, J.S.O. Evans, A.W. Sleight, J. Solid State Chem. 137 (1998) 143.
[9] I. Radosavljevic, J.S.O. Evans, A.W. Sleight, J. Solid State Chem. 141 (1998) 149.
[10] I. Radosavljevic, J.S.O. Evans, A.W. Sleight, J. Alloys Compd. 284 (1999) 99.
[11] I. Radosavljevic, A.W. Sleight, J. Solid State Chem. 149 (2000) 143.
[12] F. Abraham, M. Ketatni, G. Mairesse, B. Mernari, Eur. J. Solid State Chem. 31 (1994) 313.
[13] A. Mizrahi, J.P. Wignacourt, H. Steinnk, J. Solid State Chem. 133 (1997) 516.
[14] A. Mizrahi, J.P. Wignacourt, M. Drache, P. Conant, J. Mater. Chem. 5 (1995) 901.
[15] F. Abraham, M. Ketatni, Eur. J. Solid State Inorg. Chem. 32 (1995) 429.
[16] M. Ketatni, F. Abraham, O. Mentre, Solid State Sci. 1 (1999) 449.
[17] M. Ketatni, B. Mernari, F. Abraham, O. Mentre, J. Solid State Chem. 153 (2000) 48.
[18] M. Ketatni, O. Mentre, F. Abraham, F. Kzaiber, B. Mernari, J. Solid State Chem. 139 (1998) 274.
[19] S. Giraud, M. Drache, P. Conflant, J.P. Wignacourt, H. Steinfink, J. Solid State Chem. 154 (2000) 435.
[20] X. Xun, A. Yokochi, A.W. Sleight, J. Solid State Chem. 168 (2002) 224.
[21] F. Abraham, O. Cousin, O. Mentre, M. Ketatni, J. Solid State Chem. 167 (2002) 168.
[22] D.G. Porob, T.N. Guru Row, Acta Crystallogr. B 59 (2003) 606.
[23] A. Bruker, SMART, SAINT, Bruker AXS, Inc, Madison, WI, USA, 1998.
[24] R. Shirley, The CRYSFIRE System for Automatic Powder Indexing: User's Manual, The Lattice Press, England, 1999.
[25] G.M. Sheldrick, SHELXS97, SHELXL97, University of Göttingen, Germany, 1997.
[26] L.J. Farrugia, J. Appl. Crystallogr. 32 (1999) 837.
[27] A.C. Larson, R.B. von Dreele, Los Alomos Laboratory Report, No. LA-UR-86-748, 1987.